States at high excitation in ^{12}C from the ^{12}C(^{3}He,^{3}He)3α reaction

C. Wheldon, Tz. Kokalova, M. Freer, A. Glenn, D. J. Parker, T. Roberts, and I. Walmsley
School of Physics and Astronomy, University of Birmingham, Birmingham, B15 2TT, United Kingdom
(Received 29 May 2014; revised manuscript received 7 July 2014; published 24 July 2014)

The high excitation energy region, E_x >15 MeV, of ^{12}C was probed using the ^{12}C(^{3}He,^{3}He)3α reaction. The ^{3}He nucleus was detected using a particle identification telescope and was used to reconstruct the excitation energy of ^{12}C. The 3α decay of ^{12}C was observed via the detection of two of the three final-state α particles in an array of two double-sided silicon strip detectors. The present analysis selected decays via ^{8}Be$_{gs}$ + α. Evidence is found for a series of states at 16.3(0.2), 17.2(0.2), 18.4(0.2), 19.7(0.2), 22.2(0.3), and 25.1(0.3) MeV.

DOI: 10.1103/PhysRevC.90.014319 PACS number(s): 25.55.Ci, 21.10.Hw, 21.10.Re, 27.20.+n

I. INTRODUCTION

The nucleus ^{12}C has received a great deal of attention recently in a bid to better understand its spectroscopy and hence the underlying structure. From an experimental perspective, the states above the ^{12}C $\rightarrow$ 3α-decay threshold have proved most challenging, in part due to the broad widths of the states. It is in this region that the 7.65-MeV Hoyle state plays a significant role in both the spectroscopy and the synthesis of ^{12}C and the triple-α burning process in the red giant phase of stars [1].

Perhaps the most notable recent triumph is the experimental effort to observe the excitations of the 0^+ Hoyle state. Through a series of measurements [2–6], it has now been demonstrated that a 2^+ state exists close to 9.8 MeV, whose properties are consistent with being an excitation of the Hoyle state. Further, there is tentative evidence for a 4^+ state at 13.3 MeV [7]. High-resolution measurements have also demonstrated that a previously tabulated 2^+ state at 11.16 MeV [8,9] is likely to have been an experimental artifact [10].

Similarly, there has been progress in understanding other rotational bands in ^{12}C. A precision measurement of the width of the 9.64-MeV, 3^-, state has recently been published [11] indicating that α clustering may play a non-negligible role in the structure of this state. A collective 4^- excitation of this state has been suggested at 13.35 MeV [12,13], with a 5^- member at 22.4 MeV [14]. The rotational behavior of the ground-state rotational band and the $K^\pi = 3^-$ band (associated with the 9.64-MeV state) are indicative of a D_{3h} dynamical symmetry reflecting the underlying triangular 3α structure of ^{12}C [14].

While there has been some progress in understanding the link between the spectroscopy and structure for some of the states of ^{12}C, it is clear that this is still incomplete. For example, there are a number of measurements that indicate broad 0^+ and 2^+ resonances that cannot be placed into the above systematics [3,15]. Thus, there remains significant scope for detailed measurements that can constrain the properties of ^{12}C and these will involve techniques that range from the utilization of nuclear reactions to β decay.

From the theoretical perspective understanding the structure of ^{12}C has become something of a milestone. The ground state may be described within the framework of the shell model [16,17], but such calculations cannot reproduce the properties of the 7.65-MeV, 0^+, Hoyle state. The lack of ability of this approach to capture the properties of this state is attributed to the well-developed cluster structure. The antisymmetrized molecular dynamics (AMD) [18] and fermionic molecular dynamics (FMD) [19] methods possess greater flexibility and are able to capture both the structure of the compact shell model and clusterlike structures. Indeed, the FMD approach suggests that the Hoyle state may not be a rigid α-cluster structure but a superposition of several cluster geometries. This may be indicative of a state that resembles an α-particle gas [20,21]. The most ambitious calculations applied to ^{12}C employ chiral effective field theory [22,23]. These successfully reproduce the energy of both the ground state and the Hoyle state in ^{12}C. Though many of the more recent calculations are technically sophisticated, it is worth noting that the dynamical symmetries of ^{12}C were first suggested by Hafstad and Teller in 1938 [24] and the potential gaslike nature of states above the α-decay threshold were suggested by Uegaki and co-workers in 1977 [20], where in both cases a simple α-cluster framework was exploited.

A greatly improved understanding of the spectrum of ^{12}C up to an energy of 15 MeV has been established. However, above this energy the data compilations [8,9] are dominated by states with $T = 1$ character and states with unnatural parity [$\pi \neq (-1)^J$]. In part this is due to the opening of the proton and neutron channels at these energies. As has been recently demonstrated by the measurement of the ^{12}C(^{4}He,^{4}He)3α reaction [14], there should also exist a number of $T = 0$, natural parity, states linked to the continuation of rotational structures at lower excitation energies that have yet to be observed. In the present measurement of the ^{12}C(^{3}He,^{3}He)3α reaction we search for such states.

II. EXPERIMENTAL DETAILS

The present measurements were made at the University of Birmingham's MC40 cyclotron with a 2-enA ^{3}He beam. The integrated exposure was ~25 μC and the beam energy was 46 MeV. The beam was incident on a 300 μg cm^{-2} carbon target and collimated such that the size of the beam spot on the target was 2 mm in diameter.

The reaction that was of primary interest was ^{12}C(^{3}He,^{3}He)3α, corresponding to the inelastic excitation of ^{12}C above the 3α-decay threshold (7.275 MeV). The detection system was designed to uniquely identify this reaction with

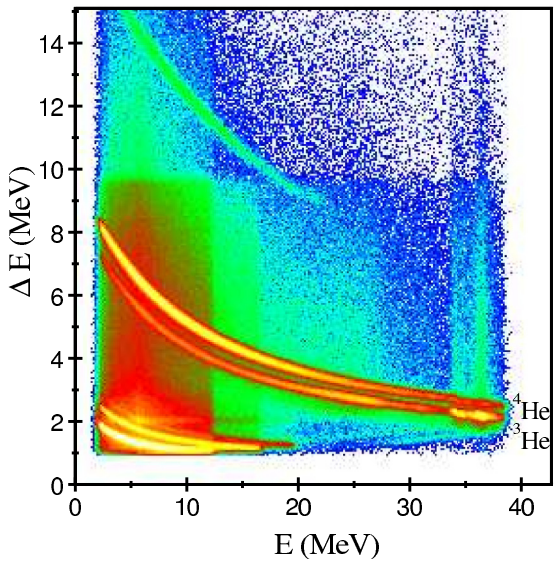

FIG. 1. (Color online) Particle identification spectrum showing loci corresponding to ^{6}Li, ^{4}He, ^{3}He, ^{2}H, and ^{1}H.

good suppression of competing channels. All of the detectors employed were double-sided silicon strip detectors (DSSSDs). These had a surface area of 5 × 5 cm^2 segmented into 16 strips on both sides of the wafer. These strips were such that on one face they had a vertical orientation, while on the other the strips were horizontal. This effectively subdivided the detector into 256 quasi-independent pixels. This segmentation permitted the energies and angles of all of the detected particles to be recorded and hence their momenta determined. These detectors were calibrated using a 3-line α source and had a typical energy resolution [full width at half maximum FWHM)] for each strip of 50 keV.

To uniquely identify the inelastically scattered ^{3}He, two DSSSDs were formed into a particle identification telescope. The first element was 70 μm thick (ΔE) and the second was a 1-mm-thick detector (E). The characteristic particle identification spectrum, achieved using the telescope, is shown in Fig. 1. This spectrum shows the loci of nuclei from ^{1}H to ^{6}Li, with those for ^{3}He and ^{4}He being well resolved. This telescope was placed 9.8 cm from the target (front detector) at an angle of 32.5°, with the two detectors in the telescope being separated by 1.3 cm.

To detect the decay products from the inelastically excited ^{12}C nucleus, two further DSSSDs were placed on the opposite side of the beam axis to the detector telescope; these were at 11.5 and 9.8 cm from the target at angles of 27.5° and 57.5°, respectively. These were both 500 μm thick, again with active areas of 5 × 5 cm^2 subdivided into 16 strips on both faces. The reaction trigger was set to record events in which there was a threefold multiplicity summed over the three thicker detectors.

Complete kinematic reconstruction of the ^{12}C(^{3}He,^{3}He)3α reaction is possible through the measurement of three of the four final-state particles. In the present analysis, events in which ^{3}He was detected in the telescope in coincidence with at least two recorded particles in the two detectors on the opposing side of the beam axis were reconstructed. In particular, given that the decay of ^{12}C predominantly proceeds through the intermediate step ^{8}Be + α, the first step in the analysis was to reconstruct the decay energy of ^{8}Be from these two detected particles. This is equivalent to calculating the relative energy of the two α particles,

$$E_{\rm rel} = E_1 + E_2 - E_{^8{\rm Be}}, \tag{1}$$

where E_1 and E_2 are the energies of the two detected particles and $E_{^8{\rm Be}}$ is the kinetic energy of the ^{8}Be nucleus prior to decay. This latter quantity was calculated based on the assumption that the two detected particles were α particles and using the principle of conservation of momentum:

$$\mathbf{p}_{^8{\rm Be}} = \mathbf{p}_1 + \mathbf{p}_2. \tag{2}$$

Here $\mathbf{p}_{^8{\rm Be}}$ is the momentum of the ^{8}Be nucleus reconstructed from the momenta of the two α particles $\mathbf{p}_1$ and $\mathbf{p}_2$. Hence,

$$E_{^8{\rm Be}} = \frac{\mathbf{p}_{^8{\rm Be}} \cdot \mathbf{p}_{^8{\rm Be}}}{2m_{^8{\rm Be}}}, \tag{3}$$

$m_{^8{\rm Be}}$ being the mass of the ^{8}Be nucleus.

The resulting spectrum is shown in Fig. 2(a). The peak close to 92 keV corresponds to the decay of the ^{8}Be ground state into 2α. The events within this peak were then selected for further analysis (the limits used were 55 to 150 keV).

The full identification of the reaction of interest required the reconstruction of the Q value. Here the Q value is given

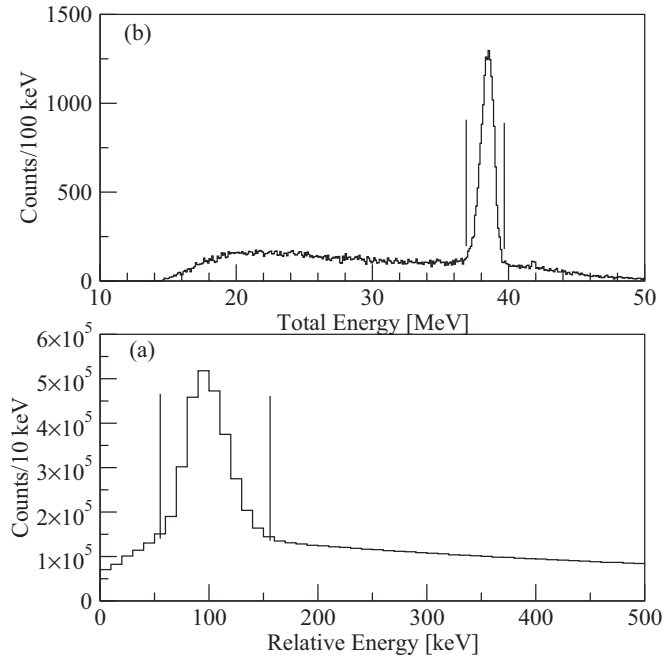

FIG. 2. (a) Two α relative energy spectrum constructed for the two detected particles in the 500-μm-strip detectors. The peak close to 92 keV corresponds to the decay of the ^{8}Be ground state. The two vertical lines indicate the limits used to select the events. (b) Total energy spectrum for the four final-state particles, assumed to be ^{3}He + 3α. Again, the vertical lines indicate the events selected for further analysis.

by

$$Q = E_{\rm tot} - E_{\rm beam}, \tag{4}$$

where $E_{\rm tot}$ is the sum of the kinetic energies of the four final-state particles and $E_{\rm beam}$ is the energy of the beam. $E_{\rm tot}$ is the kinetic energy of the two detected α particles and the ^{3}He nucleus, plus that of the missing, unobserved, α particle. The energy of this last particle was deduced from conservation of momentum coupled with the assumption of the mass being that of an α particle. The total energy, $E_{\rm tot}$, is shown in Fig. 2(b). The peak at 38.5 MeV (FWHM = 1.1 MeV) corresponds to the ^{3}He + 3α final state, which should occur at $46 - 7.28 = 38.72$ MeV ($E_{\rm beam} + Q$). The small difference in energy is consistent with energy losses in the target. The reaction of interest can then be selected through the placement of a software gate around the peak in this latter spectrum. The three stages of event selection employed here are thus (i) identification of ^{3}He, (ii) identification of ^{8}Be$_{\rm gs} \rightarrow 2\alpha$, and (iii) the correct reaction Q value.

The excitation energy of ^{12}C may be reconstructed either from the kinematics of the ^{3}He nucleus or from the properties of the three final-state α particles. In the present instance, the best resolution is achieved from the first of these two approaches. Figure 3 shows the calculated ^{12}C excitation energy spectra. These spectra show evidence of a number of peaks in the ^{12}C excitation energy spectrum associated with the well-known states at 7.65 MeV, 0^+; 9.64 MeV, 3^-; 10.84 MeV 1^-; and 14.08 MeV, 4^+. The experimental resolution determined from the 7.65- and 9.64-MeV states is ~530 keV (FWHM). In the present measurement the energies of these states are found to be 7.63, 9.67, 10.86, and 14.18 MeV. The first three are within 35 keV of the known energies of the states; the last is within 100 keV.

Above 14.5 MeV there appear to be a number of additional peaks extending perhaps above 25 MeV. The two sets of spectra in Figs. 3(a) and Fig. 3(b) illustrate the influence of the selection on the ground-state energy of ^{8}Be, with the gate being removed in Fig. 3(b). Aside from perhaps slightly larger background in Fig. 3(b), the structures in the spectra are very similar. This is perhaps not so surprising because the efficiency for the detection of decays proceeding via the 2^+ state in ^{8}Be would be dramatically reduced because the decay cone for this state is significantly larger than the angular range intercepted by the detectors. It should be noted that the selection of decay of ^{12}C via the ^{8}Be$_{\rm gs} + \alpha$ channel crucially selects only states with natural parity (e.g., 0^+, 1^-, 2^+, 3^-, ...).

It is possible that some of the structure that appears at higher excitation energies in the ^{12}C spectrum originates from contaminants from other reactions. Given that the final-state comprises ^{3}He + ^{8}Be$_{\rm gs}$ + ^{4}He, this may be reached from reactions producing ^{7}Be $\rightarrow$ ^{3}He + ^{4}He and ^{11}C $\rightarrow$ ^{8}Be$_{\rm gs}$ + ^{3}He. Figure 4 shows the excitation energy of ^{7}Be (calculated from the kinematics of ^{8}Be$_{\rm gs}$) plotted against the excitation energy of ^{12}C calculated from the ^{3}He nucleus. This latter spectrum shows that the region probed lies at very high excitation energies in ^{7}Be and hence is an unlikely source for the events.

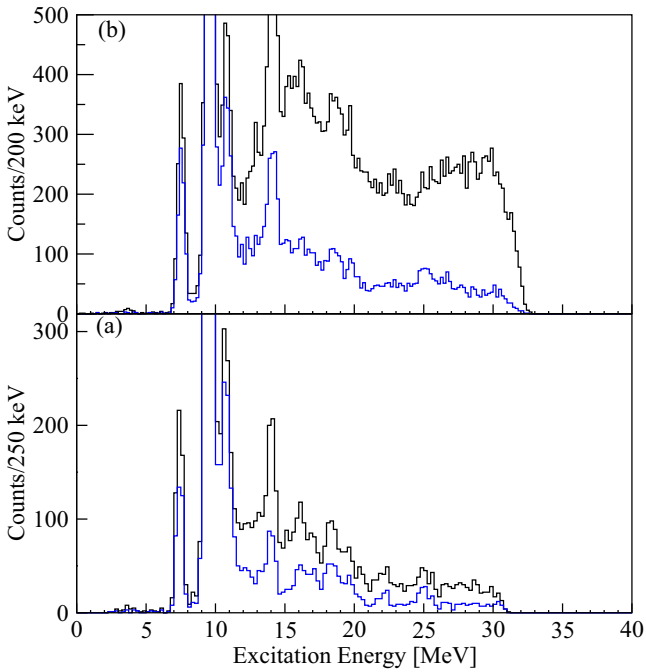

FIG. 3. (Color online) (a) Carbon-12 excitation energy spectrum for the ^{12}C(^{3}He,^{3}He)3α reaction (black line) for events where two of the α particles came from the decay of the ^{8}Be ground state and fell within the gate applied to the $E_{\rm tot}$ spectrum (Fig. 2). The events associated with the subset within the window shown in Fig. 4 are shown by the blue (gray) histogram. (b) The same as in panel (a) but with the condition that two of the α particles arise from the decay of ^{8}Be$_{\rm gs}$ removed.

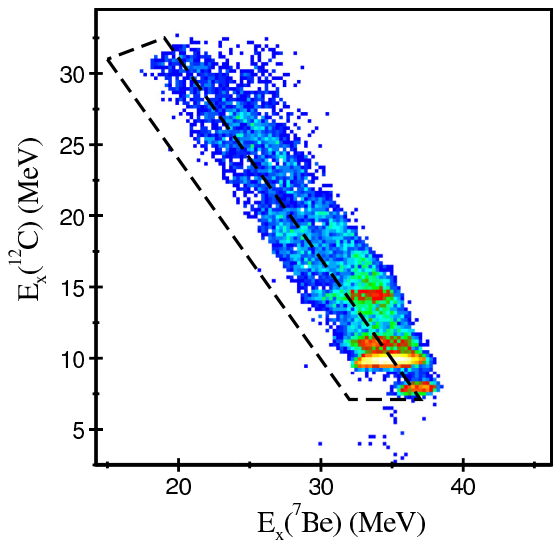

FIG. 4. (Color online) Dalitz plot showing the reconstruction of the excitation energy of ^{7}Be plotted against that of ^{12}C. The excitation energy of ^{7}Be was reconstructed from the properties of the ^{8}Be nucleus, and the excitation energy of ^{12}C was reconstructed from the detected ^{3}He. Events associated with the decay of states in ^{11}C into ^{8}Be + ^{3}He should lie on diagonal loci (negative gradient). There is some evidence of such a contribution passing through the coordinates [E_x(^{7}Be), E_x(^{12}C)] = [30 MeV, 18 MeV]. The dashed-line box indicates the region selected shown in Figs. 3 and 5.

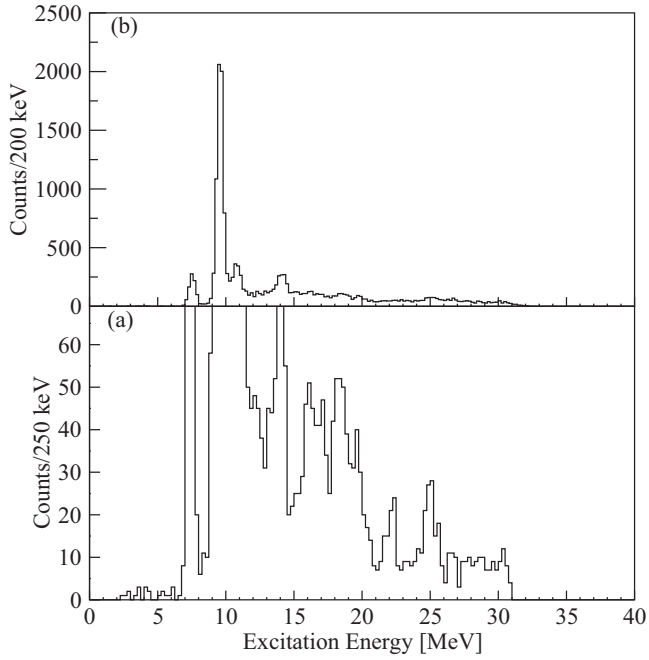

FIG. 5. The ^{12}C excitation energy spectra with all of the selection criteria, designed to remove background, applied. Panel (a) shows a vertically expanded view of panel (b). The slightly different binning (200 and 250 keV) is used due to the lower statistics in the higher energy region displayed in panel (a).

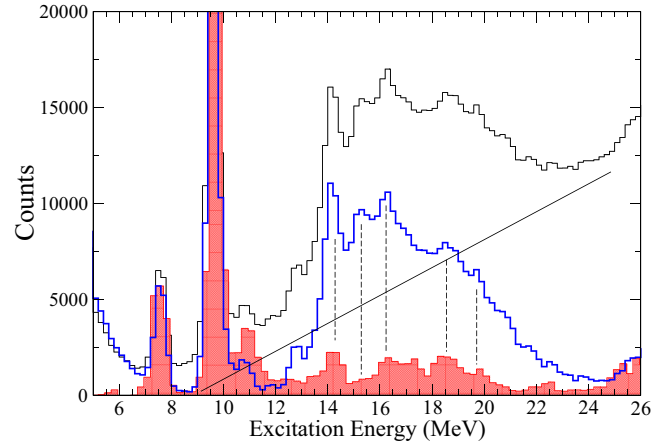

FIG. 6. (Color online) Comparison between the ^{12}C excitation energy spectrum for all events and those in coincidence with ^{8}Be$_{gs}$. The black histogram (largest amplitude histogram at $E_x = 16$ MeV) corresponds to the calculated singles ^{12}C excitation energy spectrum for all ^{3}He nuclei detected. The blue (gray) histogram is after a linear background has been subtracted (background is shown by the straight line). The red-shaded histogram corresponds to events decaying to the ^{8}Be ground state corrected for detection efficiency—see the text for details. The vertical dashed lines indicate the states for which branching ratios have been estimated.

On the other hand there is evidence for some structure with a diagonal locus with a negative gradient. Such events would be associated with the decay of states in ^{11}C in the energy interval $E_x(^{11}\mathrm{C}) = 15$ to 20 MeV. A similar spectrum with the ^{8}Be$_{gs}$ condition removed shows this locus more strongly. To remove this potential component which would present a background in the ^{12}C excitation energy spectrum, the events within the region indicated by the dashed-line box in Fig. 4 were selected. These are shown by the blue (gray) histograms in Fig. 3.

The effect of this latter gate is to accentuate the structure in the spectra, demonstrating the removal of the background component, and strongly suggests the presence of states at high excitation in ^{12}C. The "final" ^{12}C excitation energy spectra are shown in Fig. 5 with two different vertical scales.

To estimate the branching ratios for the decay of the ^{12}C excited states for the decay to ^{8}Be$_{gs} + \alpha$ the ^{12}C excitation energy spectrum has been calculated from the detected ^{3}He nuclei, with and without the detection of ^{8}Be$_{gs}$ in coincidence (see Fig. 6). The "singles" excitation energy spectrum contains significant background that increases towards higher excitation energies. This has been estimated using a linear fit (the straight line in Fig. 6) and then subtracted from the singles spectrum [blue (gray) line in Fig. 6]. There are a number of states between 14 and 21 MeV that can clearly be identified in this spectrum. The ^{12}C excitation energy spectrum for the ^{8}Be$_{gs}$ coincidences has been corrected for the acceptance cut used in Fig. 4 and the variation in the detection efficiency for the coincidence detection of ^{8}Be$_{gs}$. This detection efficiency was calculated using Monte Carlo simulations of the reaction and detection geometries assuming isotropic distributions for the particle emission. This latter assumption introduces only a small (20%) uncertainty in the relative efficiencies.

Finally, the corrected ^{12}C, ^{8}Be$_{gs}$-gated, excitation energy spectrum was normalized such that its amplitude was 97% of that of the 9.64-MeV peak in the singles spectrum; the 9.64-MeV, 3^-, state is known to have a 97% α_0-decay branch [12].

The results (Table I) show that the α_0 branching ratio for the 7.65-MeV state is 100%, as expected, but that for the 10.8-MeV, 1^-, state is clearly overestimated due to the limitations of the background parametrization in this region. At higher energies the α_0 branching ratio for the 14.2-MeV peak, which corresponds to the 14.1-MeV, 4^+, state, has a calculated α_0 branching ratio of 20(10)%. This is very close to the 17% that may be inferred from the measurements reported in Refs. [12,25]. Due to the assumptions in the Monte Carlo calculations and background subtraction, uncertainties in the present branching ratios for the region above 14 MeV are estimated to be as large as a factor of 2.

III. RESULTS AND DISCUSSION

At excitation energies above 20 MeV there appears to be two clear peaks at 22.2(0.3) and 25.1(0.3) MeV. These are seen in both spectra in Fig. 3(a) [black lines and blue (gray) lines]. The uncertainties are based on an extrapolation of the deviations, between the energies measured here and tabulations, at lower excitation energy in the present measurements. It is difficult to extract the α_0 branching ratios for these states as

TABLE I. Carbon-12 excited states above 14 MeV observed in the present measurements compared with those populated in reactions including ^{3}He inelastic scattering measurements (Table 12.19 in Ref. [9]) and those populated in the ^{11}B + p reaction (Table 12.11 in Ref. [9]).

Present			Table 12.19 in Ref. [9]			Table 12.11 in Ref. [9]			
E_x (MeV)	Γ (MeV)	$\Gamma_{\alpha 0}/\Gamma$	E_x (MeV)	Γ (MeV)	$J^\pi;T$	E_x (MeV)	Γ (MeV)	$J^\pi;T$	$\Gamma_{\alpha 0}/(\Gamma_{\alpha 0}+\Gamma_{\alpha 1}+\Gamma_p)$
14.2(0.2)	<0.6	0.20(0.10)	14.08(0.03)		$4^+;0$				
15.2(0.2)	<0.6	<0.08	15.11		$1^+;1$				
16.3(0.2)	<0.6	0.18(0.10)	16.11		$2^+;1$	16.1058	0.0053	$2^+;1$	0.055(0.011)
17.2(0.2)	<0.6		17.230	1.15	$1^-;1$				
18.4(0.2)	<0.8	0.25(0.10)	18.40(0.06)	0.4(0.1)	$(2^+);1$	18.38	≃0.4	$3^-;1$	0.21
19.7(0.2)	<0.6	0.21(0.10)	19.56(0.05)	0.25	$(1,2,3)^+$				
22.2(0.3)	<0.7		22.4(0.1)	0.25	$(2)^+$	22.1	0.5		
25.1(0.3)	<0.8								

there is no clear evidence for them in the singles spectrum in Fig. 6.

In the ^{8}Be$_{gs}$-gated spectrum, at energies between 15 and 20 MeV, there appears to be at least two strong peaks at 16.3(0.2) and 18.4(0.2) MeV with possible evidence for further peaks at 17.2(0.2) and 19.7(0.2) MeV. There is a further peak in the singles spectrum at 15.2 MeV that is not found in the ^{8}Be$_{gs}$-gated spectrum.

An analysis of the angular distributions provided no clear information on the nature of the spins of these states. This is most likely due to the fact that the presence of the nonzero spin of ^{3}He leads to a number of competing orbital angular momenta in the reaction, degrading oscillatory structure in the angular distributions. However, the restriction to the ^{8}Be$_{gs}$ decay channel limits the states to possessing natural parity. This would suggest that the peak at 15.2 MeV is unnatural parity (see Fig. 6) and is in fact the well-known 15.1-MeV, 1^+, $T = 1$, state [9].

There are a number of states already known between 16 and 21 MeV, which are tabulated in Refs. [8,9]. The state that is closest in energy to the present 16.3-MeV peak is at 16.11 MeV, $J^\pi = 2^+$, $T = 1$. This has a measured α_0-decay branch of approximately 5% (Table 12.11 in Ref. [8]) and hence is probably the present state. The 16.1-MeV state is known to be isospin mixed [9,26] and hence could appear in the α_0 channel. The nearby 16.57-MeV, $J^\pi = 2^-$, $T = 1$, unnatural parity state would not be expected to decay via the α_0 channel. The 18.35-MeV, J^π=3$^-$, $T = 1$, state (main table in Ref. [9]) has a tabulated 20% α_0 branch (18.38 MeV in Table 2.11 in Ref. [9]) that could perhaps be the 18.4-MeV peak seen in the present data. Given the consistently low α_0 branching ratios, it is likely that the majority of the states populated between 15 and 21 MeV are of a $T = 1$ character. Analogs of these $T = 1$ states have been strongly populated in ^{12}C(p,n)^{12}N [27] and ^{12}C(n,p)^{12}B [28] and are states with shell-model-like character [29].

The α_0 branches measured here also indicate isospin mixing for the other $T = 1$ states. On the other hand, it would appear that the 22.2- and 25.1-MeV peaks are enhanced relative to the lower energy states in the α_0 channel, which may point to a $T = 0$ character. The only other state that has a possible $T = 0$ character is the 19.7-MeV peak in the present measurements, because it has not been explicitly linked with the $T = 1$ character in previous measurements. Recent measurements have shown [14] there to be a 22.4(0.2)-MeV state in ^{12}C, which decays to ^{8}Be$_{gs} + \alpha$ with a probable spin and parity of 5^-, believed to be connected to the $K^\pi = 3^-$ band. The present peak at 22.2(0.3) MeV is probably associated with this state, providing confirmation of its relatively strong decay to the ^{8}Be$_{gs} + \alpha$ channel.

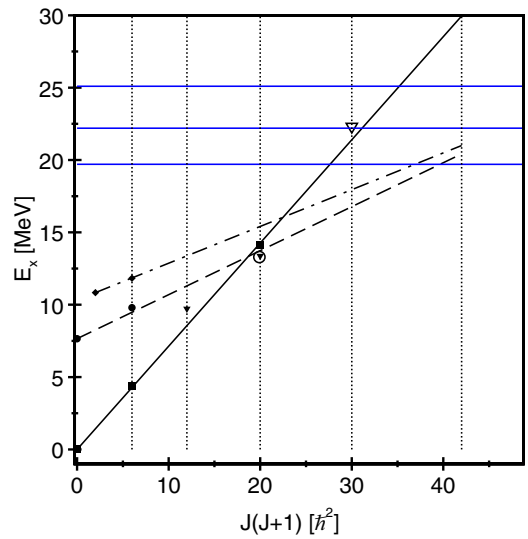

FIG. 7. (Color online) Systematics of states in ^{12}C organized according to their rotational characteristics. The solid black line (solid squares) corresponds to the ground-state rotational band: 0 MeV, 0^+; 4.4 MeV, 2^+; and 14.1 MeV, 4^+ [9]. The black dashed line is the assumed rotational band associated with the Hoyle state (solid circles are confirmed states [6] and the open circle is the possible 4^+ state [7]): 7.65 MeV, 0^+; 9.8 MeV, 2^+; and 13.3 MeV, 4^+. The K^π states at 9.64 MeV, 3^-; 13.3 MeV 4^-; and 22.4 MeV, 5^- [14] are shown by the triangles—the open triangle is for an unconfirmed assignment). The diamonds and dot-dashed line show the systematics associated with the 10.84-MeV, 1^-, state and the 11.83-MeV, 2^-, state. The blue horizontal lines indicate the energies of the possible $T = 0$ states observed in the present data: 19.7, 22.2, and 25.1 MeV.

Figure 7 shows the $T = 0$ energy-spin systematics of many of the states associated with ^{12}C and their characterization in terms of rotational bands. The horizontal lines are associated with the excitation energies of the $T = 0$ peaks in the present data. Aside from the 22.2-MeV peak there is no obvious association with the compact structures that may be linked to the ground-state band. It is possible that the state at 19.7 MeV is associated with the higher spin (5, 6) members of the more deformed structures (e.g., linked to the Hoyle state) or are associated with alternative ^{12}C structures and lower spins. It is not obvious how to place the 25.1-MeV state in terms of the current systematics. However, given its reasonably strong excitation, which is comparable to the 22.2-MeV state, it is possible that it is a strongly collective excitation.

IV. SUMMARY AND CONCLUSIONS

Measurements of the ^{12}C(^{3}He,^{3}He)3α reaction have been performed using a particle identification telescope to uniquely identify the inelastically scattered ^{3}He nucleus and two DSSSDs to reconstruct the $^8\mathrm{Be}_{\mathrm{gs}} + \alpha$ decay of excited states in ^{12}C. The measurements found evidence for the excitation of a number of states between 16 and 26 MeV that decay to this final state, specifically at excitation energies of 16.3(0.2), 17.2(0.2), 18.4(0.2), 19.7(0.2), 22.2(0.3), and 25.1(0.3) MeV. The observed state at 22.2(0.3) MeV supports the earlier observation of a state at 22.4 MeV in the ^{12}C(^{4}He,^{4}He)3α reaction. A further measurement to determine the decay branch to the $^8\mathrm{Be}_{2^+} + \alpha$ channel and the spins of the states is crucial to understanding their underlying structure.

[1] F. Hoyle, Astrophys. J. Suppl. Ser. **1**, 121 (1954).
[2] M. Itoh *et al.*, Nucl. Phys. A **738**, 268 (2004).
[3] M. Itoh *et al.*, Phys. Rev. C **84**, 054308 (2011).
[4] M. Freer *et al.*, Phys. Rev. C **80**, 041303(R) (2009).
[5] W. R. Zimmerman, N. E. Destefano, M. Freer, M. Gai, and F. D. Smit, Phys. Rev. C **84**, 027304 (2011).
[6] W. R. Zimmerman *et al.*, Phys. Rev. Lett. **110**, 152502 (2013).
[7] M. Freer *et al.*, Phys. Rev. C **86**, 034320 (2012).
[8] F. Ajzenberg-Selove, Nucl. Phys. A **336**, 1 (1980).
[9] F. Ajzenberg-Selove, Nucl. Phys. A **506**, 1 (1990).
[10] F. D. Smit, F. Nemulodi, Z. Buthelezi, J. Carter, R. W. Fearick, S. V. Förtsch, M. Freer, H. Fujita, M. Jingo, C. O. Kureba, J. Mabiala, J. Mira, R. Neveling, P. Papka, G. F. Steyn, J. A. Swartz, I. T. Usman, and J. J. van Zyl, Phys. Rev. C **86**, 037301 (2012).
[11] Tz. Kokalova, M. Freer, Z. Buthelezi, J. Carter, R. W. Fearick, S. V. Förtsch, H. Fujita, R. Neveling, P. Papka, F. D. Smit, J. A. Swartz, and I. Usman, Phys. Rev. C **87**, 057307 (2013).
[12] M. Freer *et al.*, Phys. Rev. C **76**, 034320 (2007).
[13] O. S. Kirsebom *et al.*, Phys. Rev. C **81**, 064313 (2010).
[14] D. J. Marín-Lámbarri, R. Bijker, M. Freer, M. Gai, Tz. Kokalova, D. J. Parker, and C. Wheldon, Phys. Rev. Lett. **113**, 012502 (2014).
[15] S. Hyldegaard *et al.* Phys. Rev. C **81**, 024303 (2010).
[16] S. Karataglidis, P. J. Dortmans, K. Amos, and R. de Swiniarski, Phys. Rev. C **52**, 861 (1995).
[17] P. Navrátil, J. P. Vary, and B. R. Barrett, Phys. Rev. Lett. **84**, 5728 (2000).
[18] Y. Kanada-Enyo, Prog. Theor. Phys. **117**, 655 (2007).
[19] M. Chernykh, H. Feldmeier, T. Neff, P. von Neumann-Cosel, and A. Richter, Phys. Rev. Lett. **98**, 032501 (2007).
[20] E. Uegaki, S. Okabe, Y. Abe, and H. Tanaka, Prog. Theor. Phys. **57**, 1262 (1977).
[21] Y. Funaki, H. Horiuchi, W. von Oertzen, G. Röpke, P. Schuck, A. Tohsaki, and T. Yamada, Phys. Rev. C **80**, 064326 (2009).
[22] E. Epelbaum, H. Krebs, T. A. Lähde, D. Lee, and Ulf-G. Meißner, Phys. Rev. Lett. **109**, 252501 (2012).
[23] E. Epelbaum, H. Krebs, D. Lee, and Ulf-G. Meißner, Phys. Rev. Lett. **106**, 192501 (2011).
[24] L. R. Hafstad and E. Teller, Phys. Rev. **54**, 681 (1938).
[25] D. D. Caussyn, G. L. Gentry, J. A. Liendo, N. R. Fletcher, and J. F. Mateja, Phys. Rev. C **43**, 205 (1991).
[26] J. A. Templon *et al.*, Phys. Lett. B **413**, 253 (1997).
[27] B. D. Anderson, L. A. C. Garcia, D. J. Millener, D. M. Manley, A. R. Baldwin, A. Fazely, R. Madey, N. Tamimi, J. W. Watson, and C. C. Foster, Phys. Rev. C **54**, 237 (1996).
[28] F. P. Brady *et al.*, Phys. Rev. C **43**, 2284 (1991).
[29] R. S. Hicks, J. B. Flanz, R. A. Lindgren, G. A. Peterson, L. W. Fagg, and D. J. Millener, Phys. Rev. C **30**, 1 (1984).